

Effects Due to and Derived from Spontaneous Ordering in III-V Semiconductor Alloys

Yong Zhang* and A. Mascarenhas

National Renewable Energy Laboratory, 1617 Cole Boulevard Golden, CO 80401, USA

[*yzhang@nrel.gov](mailto:yzhang@nrel.gov)

ABSTRACT

Two interesting and important aspects of spontaneous CuPt ordering in III-V semiconductor alloys, which have only been investigated recently, are reviewed in this paper. The first aspect addresses the statistical effects that should be considered as the most unique consequence of the phenomenon of ordering, more specifically, how ordering affects the alloy fluctuations and hence the physical properties of the alloy. The second aspect tackles some intriguing properties of the domain twins of two CuPt ordered variants, specifically, considering the transmission of a ballistic electron beam through such a domain twin and its analogy to a highly interesting phenomenon, negative refraction, for light.

INTRODUCTION

Spontaneous ordering in III-V semiconductor alloys has been studied for close to two decades. Despite the fact that the underlying mechanism for initiating the ordering during the epitaxial growth still remains controversial,¹⁻³ a great deal of understanding toward the consequences of ordering has been achieved, especially for the CuPt ordering in the prototype system $\text{Ga}_x\text{In}_{1-x}\text{P}$ ($x \sim 0.5$).^{4, 5} The so-called CuPt ordered structure is a mono-layer superlattice along one of the [111] directions of the cubic lattice with alternating Ga-rich and In-rich layers: $\text{Ga}_{0.5+\eta/2}\text{In}_{0.5-\eta/2}\text{P}$ and $\text{Ga}_{0.5-\eta/2}\text{In}_{0.5+\eta/2}\text{P}$, with η being the order parameter varying from 0 (full random) to 1 (full ordered). Experimentally, by empirically adjusting the growth parameters, the order parameter is found to be tunable from $\eta \approx 0$ to $\eta \sim 0.6$.⁶ Note that even though the maximum order parameter achieved so far is still not close to $\eta = 1$, it is actually higher than that reported for artificially ordered structures, e.g., GaAs/AlAs-[001] mono-layer superlattices.⁷

Beside the effort in attempting to reveal the mechanism for the formation of ordering, a vast amount of studies have been devoted to explore the effects of ordering. The most extensively investigated area is the modifications in the band structure properties due to or related to the symmetry change as a result of ordering.^{4, 5} These properties are usually obtained by averaging the corresponding properties over a large volume probed by a given experimental technique. These macroscopic effects of ordering may include, for instance, band gap reduction, valence band splitting, changes in both conduction and valence band effective masses, optical anisotropy, band offsets with respect to other semiconductors, phonon modes, etc. Although these effects are critically important for understanding the ordering process and device applications, their underlying physics in fact often shares some similarity with that of other types of perturbations, say, uniaxial stress and quantum confinement. The unique feature and the kernel of the ordering phenomenon should be the statistical aspect of ordering with alloy fluctuations continuously tunable by changing the order parameter. This aspect has not received much attention until recently when the improvement in sample quality and theoretical modeling capability has made

studies in this area feasible.^{8, 9} We will summarize the recent activities, both experimental and theoretical, of this interesting area in the first part of this paper.

Effects of ordering which have been investigated in the past have included those not necessarily intrinsic to CuPt ordering.⁴ By intrinsic we mean those properties which are not obscured by the existence of complex domain structures in the sample. Such domain structures might include, for instance, ordered domain twins, antiphase domain boundaries, and any other types of additional modulations. A few years ago, we demonstrated that ordered GaInP samples with quasi-periodically stacked ordered domain twins might behave distinctly different from those with only one ordered variant.⁴ In fact, such samples show effects resembling those predicted for a novel superlattice, termed an orientational superlattice.^{10, 11} For such a semiconductor superlattice, the quantum confinement effect is realized by periodically flipping the orientations of the symmetry axes of the constituent domains, without the need for the existence of either a band offset or an effective mass discontinuity which are normally required for a conventional semiconductor superlattice (e.g., GaAs/AlGaAs). Recently, we have discovered a few new and exciting properties associated with the transmission of a ballistic electron beam through a single ordered domain twin.¹² Because of the similarity in their wave-like properties, the results for electrons have been extended to light refraction at a domain twin of a uniaxial crystal. In the past few years, there has been a great deal of interest in the field of negative refraction. Negative refraction, as opposed to normal (positive) refraction, refers to the unusual situation of refraction of light at a material boundary when the refracted beam stays on the same side of the interface normal as the incident beam. Negative refraction was hypothesized by Veselago¹³ in the 1960' to occur when the refractive index of one of the two materials on either side of the interface became negative. Only until recently, negative refraction has been demonstrated experimentally at the interface of air and a metamaterial (which can be either an array of metallic ring and rods or photonic lattices).¹⁴⁻¹⁶ It turns out that the ordered domain twins can be used to easily generate negative refraction but with no reflection loss, not only for electrons but also for light. The second part of this paper will discuss these results.

STATISTICAL EFFECTS OF TUNABLE ORDERING

Alloy fluctuation results in a broadened energy spectrum in any semiconductor alloy, which typically manifests as a linewidth broadening for either band edge excitonic emission or absorption. One would expect that ordering should reduce the photoluminescence (PL) linewidth of the band edge excitonic transition from that of the disordered alloy. However, in reality, the linewidth of an ordered sample was often found to increase rather than decrease in the early stage of ordering studies, because the ordered samples often were of inferior quality (e.g., with smaller crystalline domain sizes) when compared to a "good" disordered sample. Only after growth conditions were optimized to yield high quality ordered samples, the expected trend, the monotonic linewidth narrowing with increasing order parameter, was finally observed in the region of η up to ~ 0.5 .⁸ A quantitative modeling for such a statistical effect has since been performed.⁹

We use a large supercell of nearly 3500 atoms to simulate the partially ordered $\text{Ga}_{0.5}\text{In}_{0.5}\text{P}$ alloy with order parameter η varying from 0 to 1. Statistical effects are accounted for by averaging over 100 configurations for each value of η . An empirical pseudopotential method is used for the band structure calculations, which has been shown to be capable of yielding a very accurate average band gap for the partially ordered alloy.⁶ A valence force field method is used

for determining the relaxed atomic configurations and the corresponding structural properties. Since CuPt ordering occurs in the [111] direction with alternating Ga-rich and In-rich atomic planes, an orthorhombic supercell is built with three cell vectors \mathbf{a}_1 , \mathbf{a}_2 and \mathbf{a}_3 along the $x' \sim [11\bar{2}]$, $y' \sim [\bar{1}10]$ and $z' \sim [111]$ direction, respectively. For a partially ordered structure, each cation layer is randomly occupied by Ga or In with probabilities $p_{\text{Ga}} = x + \eta/2$ for the Ga-rich plane and $p_{\text{Ga}} = x - \eta/2$ for the Ga-poor plane, and the total number of Ga atoms is constrained by the composition $x = 0.5$.

Fig.1 shows the histogram plots for the band gap as well as the band edge energies of the valence band and conduction band of 100 randomly generated configurations. As expected, on increasing η , the fluctuations of these quantities decrease. It is interesting to note that the main contribution to the band gap fluctuation is from the conduction band for the GaInP alloy, which can be comprehended in terms of the fact that the major part of the band gap difference between GaP and InP lies in their conduction band and that the conduction band has a smaller effective mass than that of the valence band. The information for the band gap fluctuation is most relevant for various optical measurements (e.g., emission and absorption), but that for individual band edges is more relevant for specific transport measurements related to either electrons or holes.

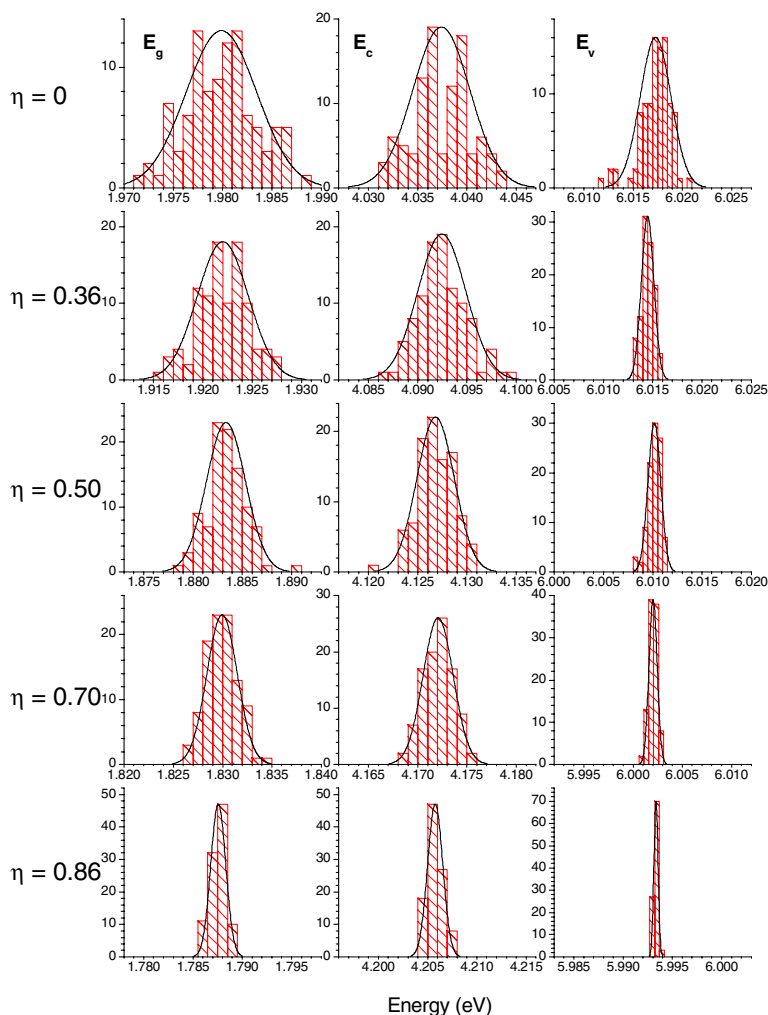


Figure 1. Histogram plots of the energy distributions of the band gap (E_g), conduction band edge (E_c) and valence band edge (E_v) for partially ordered $\text{Ga}_{0.5}\text{In}_{0.5}\text{P}$ alloys with varying order parameter η .

Fig.2(a) shows the band gap fluctuation $W_{\text{gap}}(\eta)$ (measured by the full width at half maximums of the histogram plot, FWHM), compared with the experimental data for the exciton linewidth $W_{\text{ex}}(\eta)$,⁸ as a function of η . $W_{\text{gap}}(\eta)$ not only qualitatively agrees with but also quantitatively is rather close to the experimental values of $W_{\text{ex}}(\eta)$ for $\eta < 0.55$. Nevertheless, one should notice that these two quantities are not exactly equivalent but closely related to each other. Fig.2(b) shows the fluctuation of the individual band edge: $W_c(\eta)$ for the conduction and $W_v(\eta)$ for the valence band. We would like to point out that neither the experimental data nor the calculated results, as shown in Fig.2(a), follows the widely used η^2 rule which was proposed to be a quite generally valid scaling rule.

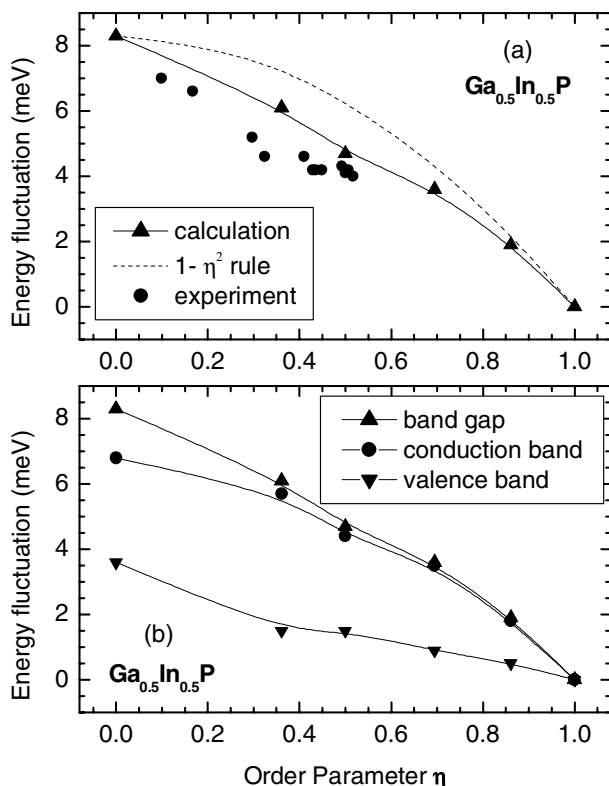


Figure 2. The energy fluctuation of the band gap $W_{\text{gap}}(\eta)$, of the conduction band edge $W_c(\eta)$, and of the valence band edge $W_v(\eta)$ for a partially ordered $\text{Ga}_{0.5}\text{In}_{0.5}\text{P}$ alloy, measured by the full width at half maximum (FWHM) of the histogram plots (shown in Fig.1), as a function of the order parameter η . (a) A comparison of the calculated $W_{\text{gap}}(\eta)$ with the low temperature PL linewidth $W_{\text{ex}}(\eta)$ and a curve predicted by a simple η^2 dependence. (b) Calculated $W_c(\eta)$, $W_v(\eta)$ as well as $W_{\text{gap}}(\eta)$.

The ordering induced statistical changes are also reflected in the bond length distributions. It is well known that for a random ternary alloy, $\text{Ga}_x\text{In}_{1-x}\text{P}$ for example, there are two average bond lengths (the so-called bimodal behavior) that are close to those of Ga-P and In-P bond in the binaries, respectively. For a CuPt ordered $\text{Ga}_{0.5}\text{In}_{0.5}\text{P}$ alloy, the average bond length for both Ga-P and In-P has been found to be different for the bonds along the ordering direction (O) and along the lateral direction (L), which in principle is detectable by polarized extended x-ray absorption fine structure, EXAFS, measurements. Fig.3 shows the typical distributions of the “O” and “L” type bonds for partially ordered $\text{Ga}_{0.5}\text{In}_{0.5}\text{P}$ with different order parameters η . The results are obtained from “representative” configurations which yield the average band gaps for each η value. As expected, the number of “O” bonds is about 1/3 the number of “L” bonds. For the random structure with $\eta = 0$, the distributions of “O” and “L” bonds are essentially the same. With increasing η , their distributions gradually start to separate from each other. However, they

remain strongly overlapped with each other for η up to 0.5 which is roughly the order parameter for the strongest ordered samples currently available.

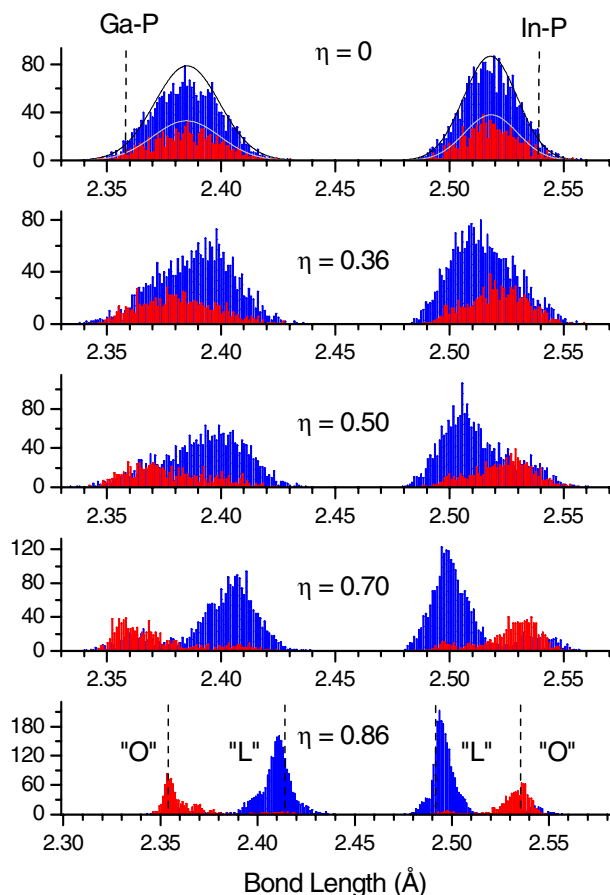


Figure 3. Histogram plots of the bond length distributions of partially ordered $\text{Ga}_{0.5}\text{In}_{0.5}\text{P}$ alloys with order parameter $\eta = 0, 0.36, 0.50, 0.70,$ and 0.86 . Blue – for the “L” type bonds along the lateral directions; Red - for the “O” type bonds along the ordering direction. The dashed vertical lines denote the Ga-P and In-P bond length in the binaries on the $\eta = 0$ panel (the up most), and in the fully ordered structure ($\eta = 1$) on the $\eta = 0.86$ panel (the bottom).

Fig.4 shows the average bond lengths and their statistical fluctuations as functions of η^2 . In agreement with the results of an earlier calculation,¹⁷ the average bond length follows the η^2 dependence very well, as shown in Fig.4(a). However, as shown in Fig.4(b), it is a surprise to find that the bond length fluctuation first increases from that for the random structure, and then, decreases after $\eta > 0.7$. Here we have taken the standard deviation of the average value as the measure of the fluctuation. This observation is counterintuitive in the sense that ordering should always reduce the random fluctuation. A qualitative explanation has been given in the original paper.⁹ There are a few significant implications of the results shown in Fig.3 and Fig.4. First, as shown in Fig.4(a), for η up to 0.5, the “O” –“L” splitting is smaller than 0.2 \AA which is the typical experimental uncertainty of any EXAFS measurements. Second, as shown in Fig.3, the strong overlap between their distributions and the 1: 3 ratio for the counts of bonds make it unfeasible to distinguish the “O” and “L” bonds by using any unpolarized EXAFS techniques, unless the samples are very highly ordered. These two points might explain why only a single average Ga-P bond length was extracted from a recent XAFS measurement of partially ordered GaInP alloys.¹⁸

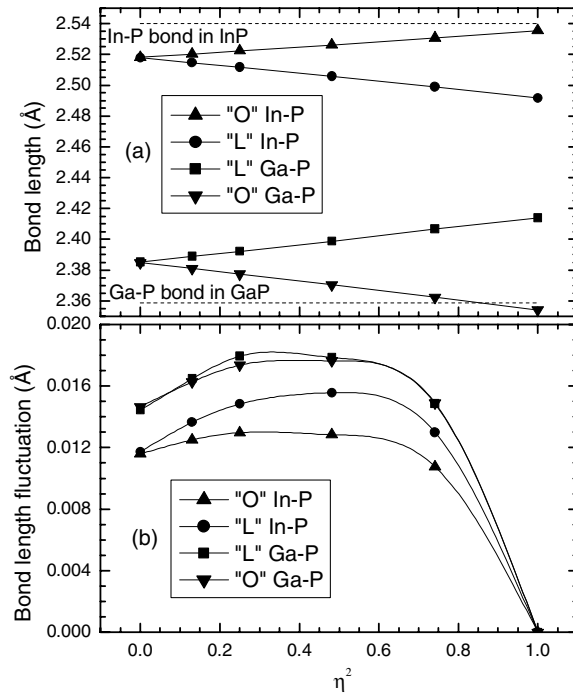


Figure 4. (a) Average bond lengths for the four types of bonds in partially ordered $\text{Ga}_{0.5}\text{In}_{0.5}\text{P}$ alloys versus η^2 ("O" – along the ordering direction, "L" – along the lateral directions). (b) Bond length fluctuations versus η^2 for the four types of bonds.

REFRACTION OF BALLISTIC ELECTRONS OF AN ORDERED DOMAIN TWIN

The transmission of an electron wave through the interface of two different semiconductors (A and B) is quite similar to the refraction of light at the interface of two materials with mismatched refractive index ($n_A \neq n_B$). Perhaps the closest analogy to the refraction of light would be the case in which the two semiconductors differ only in their effective masses ($m_A \neq m_B$). In either case, refraction inevitably is associated with a finite reflection, because of the refractive index or effective mass mismatch. Furthermore, for most of the commonly encountered situations in semiconductors, there will always be a band offset (i.e., an energy step) between A and B, causing an additional energy loss for the transmission across such an interface. We have shown recently¹² that it is in fact possible to have only the intended refraction, the ability to steer the beam, with no reflection loss (i.e., *total refraction*), when refraction occurs at the interface of a domain twin of anisotropic semiconductors or crystals for either a ballistic electron or a light beam.

In the past few years, the phenomenon of *negative refraction* (i.e., the incident beam being bent to the same side of the interface normal after refraction) has attracted a great deal of attention. It was first suggested by Veselago¹³ that negative refraction can occur at the interface of a normal medium, with both permittivity ϵ and permeability μ being positive, and an abnormal medium, with both ϵ and μ being negative. Until now, there is no real material (i.e., with a real crystal structure) known to simultaneously have negative ϵ and μ . Nevertheless, metamaterials with negative *effective* refractive index have been found (for example, arrays of split-ring and wires of copper¹⁹), and negative refraction has been demonstrated with these types of materials.¹⁵ Negative refraction has also been demonstrated using either dielectric¹⁴ or metallic¹⁶ photonic crystals without negative *effective* refractive index but relying on complex Bragg scattering

effects.^{20, 21} In all these approaches, negative refraction can only be realized in a small band width appropriate for the material used. Note that the structure of split-rings and rods is the only one that actually resembles the idea of Veselago but with negative ϵ and μ being *effective* index instead of the hypothetical negative index in uniform materials, and negative *effective* index can also be obtained in dielectric photonic crystals without the introduction of negative *effective* ϵ and μ .²² It has been pointed out that negative refraction can arise with just one of the four components of ϵ and μ being negative.²³ We have demonstrated¹² that the same type of interface that can yield *total refraction* for electrons and light can in fact offer *amphoteric refraction*, i.e., the refraction can be either *positive* or *negative*, depending on the angle of incidence, despite all components of the ϵ and μ being positive in the principal axes. Our findings, in principle, apply to the full spectrum of electromagnetic waves as well as ballistic electron waves. We would like to point out that the relaxation of the condition to have at least one of the components of ϵ and μ being negative in our case is because we allow the symmetry axis not to be perpendicular to the material interface.

We first consider the transmission of a ballistic electron beam at a semiconductor twin boundary, using a CuPt ordered domain twins shown in Fig.5 as a prototype system. For such a homojunction, there is obviously no band offset between the two twin components.¹¹ Thus, the two regions can simultaneously be transparent for electrons (with energy above the conduction band edge) and light (with energy below the fundamental band gap). However, the effective mass and refractive index of A and B are not matched for general directions, except for the direction of the twin plane normal. Therefore, intuitively, a finite reflection would be expected at the interface for any non-normal incidence of electron or light. However, the results are in fact counter-intuitive.

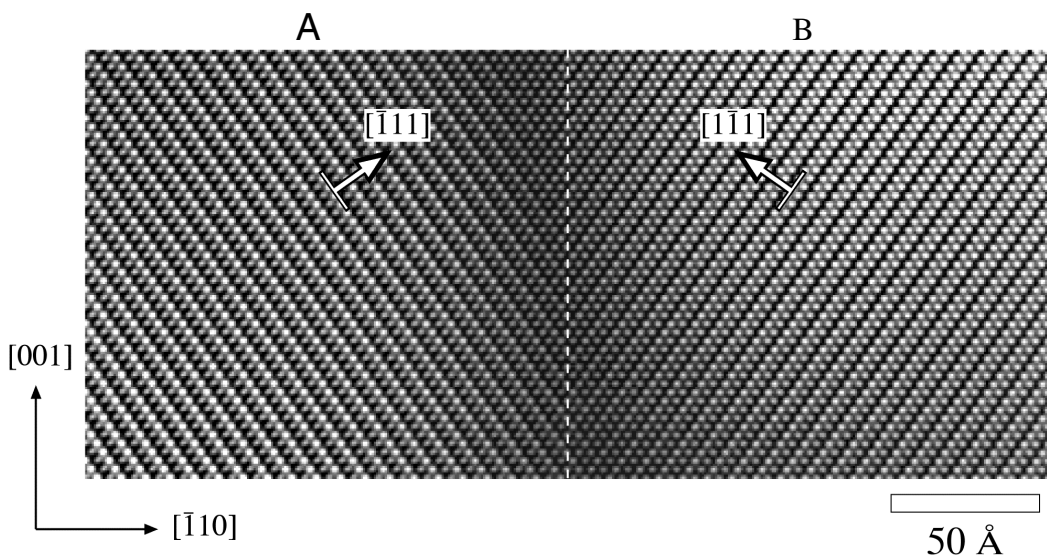


Figure 5. Electron microscopy of a domain twin. A typical high-resolution cross-sectional TEM picture of domain twin structures frequently observed in CuPt ordered III-V semiconductor alloys. The ordering directions are $[\bar{1}\bar{1}1]$ (left) and $[1\bar{1}\bar{1}]$ (right). The vertical dashed line indicates the twin boundary.

In a principal coordinate system, the effective mass tensor of the uniaxial semiconductor takes the form

$$m^{-1} = \begin{pmatrix} m_{\perp}^{-1} & 0 & 0 \\ 0 & m_{\perp}^{-1} & 0 \\ 0 & 0 & m_{\parallel}^{-1} \end{pmatrix}, \quad (1)$$

where m_{\perp} and m_{\parallel} are effective masses (in units of the free electron mass m_0) for the wave vector \mathbf{k} perpendicular and parallel to the uniaxis. In a coordinate system with z along the twin plane normal $[\bar{1}10]$, x along $[001]$, and y along $[110]$, the electron dispersion is:

$$E(\mathbf{k}) = \frac{\hbar^2}{2m_0} \left[\frac{k^2}{\bar{m}} - \gamma(k_z^2 - k_y^2) - \text{sign} 2\sqrt{2}\gamma k_x k_z \right], \quad (2)$$

where \bar{m} is the average effective mass defined as $1/\bar{m} = (2/m_{\perp} + 1/m_{\parallel})/3$, γ is the anisotropy parameter defined as $\gamma = (1/m_{\perp} - 1/m_{\parallel})/3$, $\text{sign} = +1$ for the A side, and -1 for the B side. For simplicity, we choose the x - z plane as the incidence plane (i.e., $k_y = 0$). The wavefunctions on the two sides can be written as

$$F^A(x, z) = a \exp[i(k_x x + k_{z1}^A z)] + b \exp[i(k_x x + k_{z2}^A z)], \quad (3)$$

$$F^B(x, z) = c \exp[i(k_x x + k_{z1}^B z)], \quad (4)$$

where the ‘‘a’’ term describes the incident wave, the ‘‘b’’ term the reflected wave, and the ‘‘c’’ term the transmitted wave; k_{z1}^A , k_{z2}^A , and k_{z1}^B are the solutions of Eq.2 with k_{z1}^A and k_{z1}^B corresponding to the solutions giving positive group velocity components along the z direction, while k_{z2}^A corresponding to the solution giving a negative group velocity component along the z direction. It can be shown that the boundary conditions for the continuity of the wavefunction and the current at the interface lead to two equations: $a + b = c$ and $a - b = c$. The solutions for these boundary conditions are then simply $c = a$ and $b = 0$. This surprising result implies that the twin boundary is indeed *reflectionless* and *transparent* to electron propagation. In Fig.6, the interrelation of the incident and refracted probability current density \mathbf{J} , described by the incident angle $\theta_A = \text{Arctan}(J_x^A/J_z)$ and the refraction angle $\theta_B = \text{Arctan}(J_x^B/J_z)$, is illustrated by numerical results with typical parameters achievable in III-V alloys ($\bar{m} = 0.114$, and $\gamma = 2.117$ for a fully ordered GaInP⁶). It is of particular interest to notice that it is possible to vary the incident angle from positive to negative, while keeping the refraction angle positive, i.e., the refraction can be *amphoteric*. The angle between the symmetry axis and the twin plane normal is $\theta_0 = \text{Arccos}[\sqrt{2/3}] = 35.3^\circ$ for this specific example. The maximum bending occurs with $k_x = 0$, with $\theta_{B0} = -\theta_{A0} = \sqrt{2m\gamma}/(1-m\gamma)$ ($= 24.2^\circ$). It is worth mentioning that even if one of the domains in Fig.5 is replaced by an isotropic semiconductor with an effective mass m^* , there is still a finite

range of angle of incidence in which negative refraction may happen in the anisotropic side as long as m^* satisfies a condition determined by the values of m and γ .

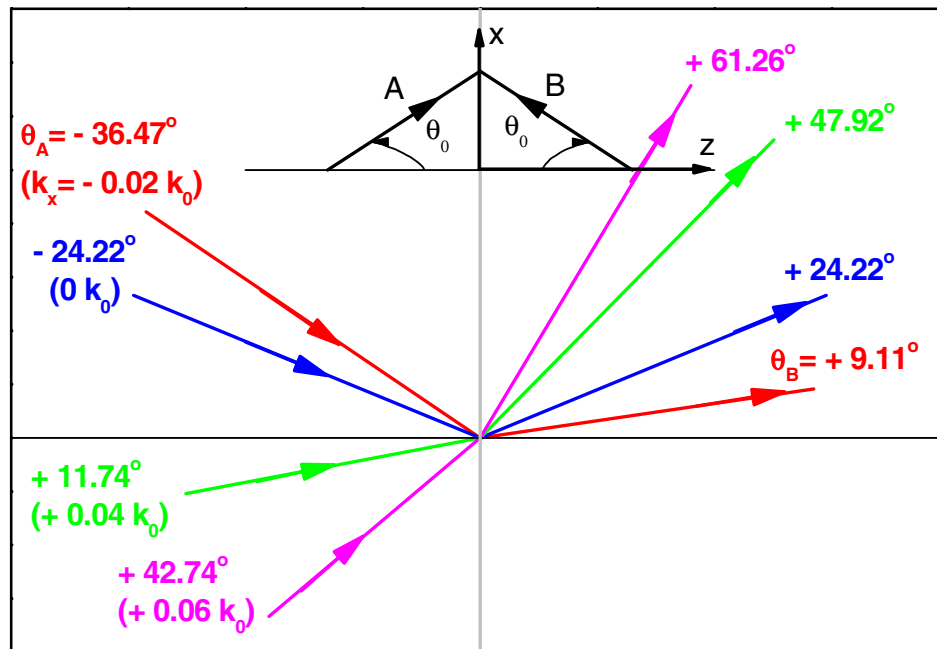


Figure 6. Refraction of a ballistic electron beam at the interface of the semiconductor twinning structure. The vertical gray line indicates the interface. Arrows A and B indicate the orientations of the uniaxis on each side with $\theta_0 = 35.3^\circ$. The beams in the two regions (left and right) can be either on the same side (corresponding to negative refraction) or on different sides (corresponding to positive refraction) of the interface normal, depending on the value of the wave vector parallel to the interface k_x (in unit of $k_0 = 2\pi/a$, a is the lattice constant of the semiconductor). The energy of the incident electron is 0.2 eV.

The above mentioned interesting effects can also occur when the ballistic electron beam is replaced with a light beam in a similar way. We next discuss the transmission of light at a twin boundary similar to that of Fig.5, but with an arbitrary angle θ_0 . Analogous to Eq.1, the dielectric tensor of an anisotropic crystal has the following form in the principal coordinate system

$$\varepsilon = \begin{pmatrix} \varepsilon_{\perp} & 0 & 0 \\ 0 & \varepsilon_{\perp} & 0 \\ 0 & 0 & \varepsilon_{\parallel} \end{pmatrix}. \quad (6)$$

It can be shown that for a wave with its electric field purely polarized along the y direction (i.e., simultaneously perpendicular to the uniaxis of the A and B side, normally viewed as an ordinary wave), the twin boundary like the one shown in Fig.5 has no effect at all on the incident wave (i.e., $\theta_A \equiv \theta_B$ with a 100 % transmission). However, for a wave with the electric field completely polarized in the incident plane x - z (normally viewed as an extraordinary wave), the effects of the

twin boundary are in fact very similar to the results obtained above for the electron beam. The dispersion relation can be obtained by solving Maxwell's equation for plane waves propagating within the x-z plane:

$$\frac{(k_z \cos \theta_0 + \text{sign} k_x \sin \theta_0)^2}{\epsilon_{\perp}} + \frac{(k_z \sin \theta_0 - \text{sign} k_x \cos \theta_0)^2}{\epsilon_{\parallel}} = \frac{\omega^2}{c^2}, \quad (7)$$

where $\text{sign} = +1$ for the A side, and -1 for the B side. We have assumed the medium is non-magnetic (i.e., the relative permeability $\mu = 1$). The electric (\mathbf{E}) and magnetic (\mathbf{H}) waves can be written for both sides in a similar manner as for Eq.3 and Eq.4, and applying the boundary conditions, we arrive at the two same equations as those for the electronic waves: $a + b = c$ due to the continuity of the tangential component of the magnetic field in the y direction, and $a - b = c$ due to the continuity of the tangential component of the electric field in the x direction, where a, b, and c are respectively the amplitude of the x component of the \mathbf{E} field for the incident, reflected and transmitted wave. Thus, we again find that the amplitude of the reflected wave is identically zero, and that of the transmitted wave always equals that of the incident wave. Similar to the situation of the electron beam, the negative refraction does occur in a range of incident angles. The largest bending or the strongest negative refraction also happens when $k_x = 0$, where the propagation direction of the light, defined by the Poynting vector $\mathbf{S} = \mathbf{E} \times \mathbf{H}$, is given as $\sin \theta_{A0} = \sin 2\theta_0 (\epsilon_{\parallel} - \epsilon_{\perp}) / (2\sqrt{\epsilon_{\perp}^2 \sin^2 \theta_0 + \epsilon_{\parallel}^2 \cos^2 \theta_0})$, and $\sin \theta_{B0} = -\sin \theta_{A0}$.

To experimentally illustrate the effect, we use an YVO₄ bicrystal with $\theta_0 = -45^\circ$ to emulate the proposed twin structure. YVO₄ is a uniaxial positive crystal with $n_o = 2.01768$ and $n_e = 2.25081$ at 532 nm. The device is formed by bonding two nominally identical crystals in optical contact. Fig.7 shows the refraction of a 532 nm laser beam at the interface of the bicrystal at two typical incident angles, which yields both positive and negative refraction. The power loss of the transmitted beam, which ideally should be zero, is measured to be in the order of 10^{-4} , due to the imperfection of the device (e.g., the relative orientation of the optical axes and the quality of the optical contact). The experiment performed here using the bicrystal for light demonstrates the feasibility of obtaining similar effects for electrons. Similar to the situation for electrons, negative refraction may even be realized with one side of the bicrystal being replaced by an isotropic material (e.g., the interface of air and an anisotropic crystal), although typically with reflection loss.²⁴

Finally, we would like to point out that the seeming counterintuitive result of zero reflection discussed above actually has a simple physical explanation that lies in the continuity condition of the normal component, $S(z)$, of the Poynting vector. In an isotropic medium, for a wave with its electric field polarized in the incident plane x-z, we have $S(z) \propto E_x^2 \sqrt{\epsilon} / \sqrt{1 - u_x^2} / \epsilon$, where $u_x = k_x c / \omega$. Obviously, if $\epsilon_A \neq \epsilon_B$, the requirement for $S_A(z) = S_B(z)$ leads to $E_{xA} \neq E_{xB}$, and thus the consequent reflection. However, for the twin structure, we have $S(z) \propto E_x^2 / \sqrt{\epsilon_0^{-1} - u_x^2} / (\epsilon_{\perp} \epsilon_{\parallel})$, where $\epsilon_0^{-1} = \epsilon_{\parallel}^{-1} \sin^2 \theta_0 + \epsilon_{\perp}^{-1} \cos^2 \theta_0$, and ϵ_0 is the refractive index for light with $k_x = 0$. Therefore, $S_A(z) = S_B(z)$ is automatically satisfied when $E_{xA} = E_{xB}$, which ensures zero reflection.

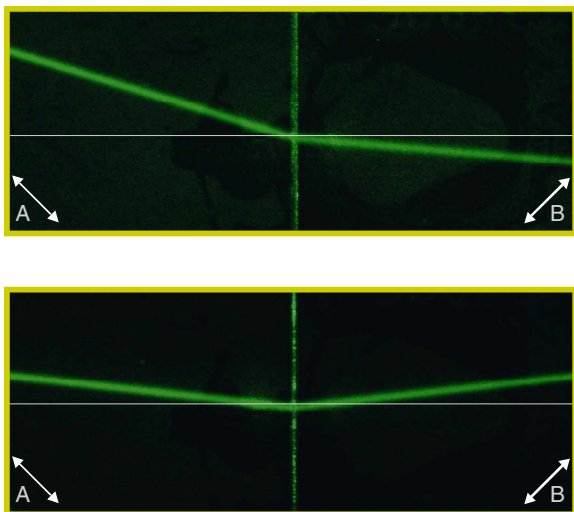


Figure 7. Images of light propagation in a YVO_4 bicrystal. The upper panel shows an example of normal (positive) refraction, the lower panel shows an example of abnormal (negative) refraction. Note that no reflection is visible at the bicrystal interface to the naked eye. The interface is illuminated by inadvertently scattered light.

CONCLUSIONS

We have offered a brief review on the effects that are either directly due to or derived from spontaneous ordering in III-V semiconductor alloys. Detailed discussions have been devoted to two relatively new areas of ordering studies: the statistical effects of tunable ordering and the interesting properties of ordered domain twins. The statistical effects are much less explored than the other effects related to ordering induced band structure changes. Perhaps the dependence of the excitonic photoluminescence linewidth on the order parameter is the only statistical feature that has been carefully studied so far. Other properties, electron and hole mobilities for instance, that are expected to strongly depend on the statistical change of the alloy fluctuations remain to be investigated in a similar manner. We have found that the ordered domain twins can serve as a zero-loss refraction mechanism for steering electron beams in electronic devices that operate in the ballistic region. They also offer a simple way for realizing the unusual phenomenon of refraction – negative refraction for both electron waves and light.

ACKNOWLEDGEMENTS

We thank collaborations with B. Fluegel, L.-W. Wang, S. P. Ahrenkiel, and M. Hanna who have made important contributions to those publications that have been summarized in this invited talk given at the MRS meeting and in this proceeding paper. This work is supported by US DOE Office of Sciences, Basic Energy Sciences.

REFERENCES

- 1 T. Suzuki, in *Spontaneous Ordering in Semiconductor Alloys*, edited by A. Mascarenhas (Kluwer Academic/Plenum Publishers, New York, 2002), p. 1.
- 2 A. G. Norman, in *Spontaneous Ordering in Semiconductor Alloys*, edited by A. Mascarenhas (Kluwer Academic/Plenum Publishers, New York, 2002), p. 45.
- 3 G. B. Stringfellow, in *Spontaneous Ordering in Semiconductor Alloys*, edited by A. Mascarenhas (Kluwer Academic/Plenum Publishers, New York, 2002), p. 99.
- 4 A. Mascarenhas and Y. Zhang, in *Spontaneous Ordering in Semiconductor Alloys*, edited by A. Mascarenhas (Kluwer Academic/Plenum Publishers, New York, 2002), p. 283.
- 5 S.-H. Wei, in *Spontaneous Ordering in Semiconductor Alloys*, edited by A. Mascarenhas (Kluwer Academic/Plenum Publishers, New York, 2002), p. 423.
- 6 Y. Zhang, A. Mascarenhas, and L. W. Wang, *Phys. Rev. B* **63**, R201312 (2001).
- 7 J. H. Li, S. C. Moss, Y. Zhang, et al., *Phys. Rev. Lett.* **91**, 106103 (2003).
- 8 Y. Zhang, A. Mascarenhas, S. Smith, et al., *Phys. Rev. B* **61**, 9910 (2000).
- 9 Y. Zhang, A. Mascarenhas, and L. W. Wang, *Phys. Rev. B* **64**, 125207 (2001).
- 10 A. Mascarenhas, Y. Zhang, R. G. Alonso, et al., *Solid State Commun.* **100**, 47 (1996).
- 11 Y. Zhang and A. Mascarenhas, *Phys. Rev. B* **56**, 9975 (1997).
- 12 Y. Zhang, B. Fluegel, and A. Mascarenhas, *Phys. Rev. Lett.* **91** (2003).
- 13 V. G. Veselago, *Sov. Phys. Usp.* **10**, 509 (1968).
- 14 H. Kosaka, T. Kawashima, A. Tomita, et al., *Phys. Rev. B* **58**, R10096 (1998).
- 15 R. A. Shelby, D. R. Smith, and S. Schultz, *Science* **292**, 77 (2001).
- 16 E. Cubukcu, K. Aydin, E. Ozbay, et al., *Nature* **423**, 604 (2003).
- 17 R. B. Capaz and B. Koiller, *Phys. Rev. B* **47**, R4044 (1993).
- 18 D. C. Meyer, K. Richter, P. Paufler, et al., *Phys. Rev. B* **59**, 15253 (1999).
- 19 D. R. Smith, W. J. Padilla, D. C. Vier, et al., *Phys. Rev. Lett.* **84**, 4184 (2000).
- 20 M. Notomi, *Opt. Quantum Electron.* **34**, 133 (2002).
- 21 C. Luo, S. G. Johnson, J. D. Joannopoulos, et al., *Optics Express* **11**, 746 (2003).
- 22 M. Notomi, *Phys. Rev. B* **62**, 10696 (2000).
- 23 I. V. Lindell, S. A. Tretyakov, K. I. Nikoskinen, et al., *Microw. Opt. Technol. Lett.* **31**, 129 (2001).
- 24 Y. Zhang, B. Fluegel, and A. Mascarenhas, unpublished. In fact, negative refraction was also observed at the interface of the bicrystal and air in our experiment.